

CFD Analysis of Electrolyte Flow Pattern in Pulse ECM and to Optimize MRR for Circular Tool

¹Anamika Mishra, ²D B Jadhav, ³P V Jadhav

¹Research scholar, Mechanical Engineering Department

²Assistant Professor, Mechanical Engineering Department

³Associate Professor, Production Engineering Department

Bharti Vidyapeeth Deemed University College of Engineering, Pune-43

E-mail- anamika_mishra@hotmail.com

ABSTRACT –ECM emerges out to be one of the major non conventional machining techniques based on Faraday's laws of electrolysis, highly efficient due to its zero tool wear characteristic. Occurrence of passivation is the major problem faced in ECM. In the present work, study of the flow pattern of electrolyte has been performed so that, the machining variable distribution can be predicted accurately thus passivation can be minimized.

A tool was modeled in Pro-E design modeler and study is considered under steady state with turbulence. The model was simulated for various inlet pressures. The results obtained showed that the flow velocity decreases when electrolyte moves towards the work piece and it increases at the outlet. Turbulent kinetic energy and turbulent eddy dissipation rate profile exhibits higher value of turbulence at pressure 1.0 kg/cm² and 1.4 kg/cm² whereas at 1.2 kg/cm² pressure, turbulence is almost negligible. The MRR is maximum affected by the tool feed rate followed by voltage and least by the electrolyte pressure. The optimize results $A_2B_2C_2$ gives the best material removal rate (MRR). Hence, from the computational simulation and experimental results it was found that 1.2 kg/cm² is a optimum value for pressure .

Keywords– PECM, CFD, Flow pattern analysis, MRR, ECM, Hole making process, CFD analysis of Electrolyte flow pattern

INTRODUCTION

Electrochemical machining is one of the most potential non conventional machining techniques used to machine high strength, heat resistant material. It is considered a reverse of electroplating, based on the principal of electrolysis. As there no contact between tool and work piece at the time of machining it results in zero tool wear. It has been widely used in the automobile industries, turbo-machinery aerospace, aeronautics, defense and medical industries because of its various advantages like negligible tool wear, high precision machining in difficult-to-cut materials, lower thermal and mechanical stress on work piece etc. Though there are few disadvantages, such as hydrogen bubble generation and its effect on Material Removal Rate (MRR), complexity of tool geometry and its effect on various process parameters, prediction of electrolyte flow pattern and its impact etc. which have been investigated by various researchers. In complicated work piece it is very difficult to know the machining variables distribution within the inter electrode gap (IEG). Study of the flow pattern of electrolyte can predict the machining variable distribution accurately and thus passivation can be avoided which is the major drawback in electrochemical machining of complicated shapes [1]. Many researchers have presented experimental and analytical studies related to material removal mechanism and current density distribution in ECM using different tool shapes and different software, but they couldn't predict the flow pattern accurately [2]. In complicated work piece, it's very difficult to deduce the machining variables within the IEG. So there is a need to understand parameters related to flow pattern. Once the flow pattern is known, then it's easy to design the tool and avoid passivation. With this background and the art of literature studied, the salient objective of the present study is

- 1) The analysis of the flow pattern of electrolyte.
- 2) Determination of the effect of various parameters over MRR (material removal rate) and surface roughness.
- 3) Optimization of results.

ELECTROCHEMICAL MACHINING SET UP

In Electrochemical Machining (ECM), a high current, low voltage DC power supply connects a conducting tool and work piece. The shaped tool is connected to the negative (-ve) terminal and work piece to the positive (+ve) which are cathode and anode respectively. A conducting electrolyte flows through a small gap that is maintained between the tool and work piece, thus providing the necessary path for electrolysis. As the direction of electron flow is from work piece to the tool, material removal is from the work piece in a reverse image of the tool. The several components of ECM setup as shown in the figure 1.

Work-Piece

Work-piece is a conducting material which acts as an anode. It is connected to the positive terminal of the pulse power supply. Generally materials with very high value of hardness or a very low value of machinability are used as work-piece materials in ECM as it removes material independent of the hardness.

Tool

Tool acting as cathode is connected to the negative terminal. Tool material used for electrochemical machining should have good electrical and thermal conductivity, easy machinability, resistance to chemicals, good stiffness and be easily obtainable. The most commonly used tool materials are copper, brass, stainless steel etc.

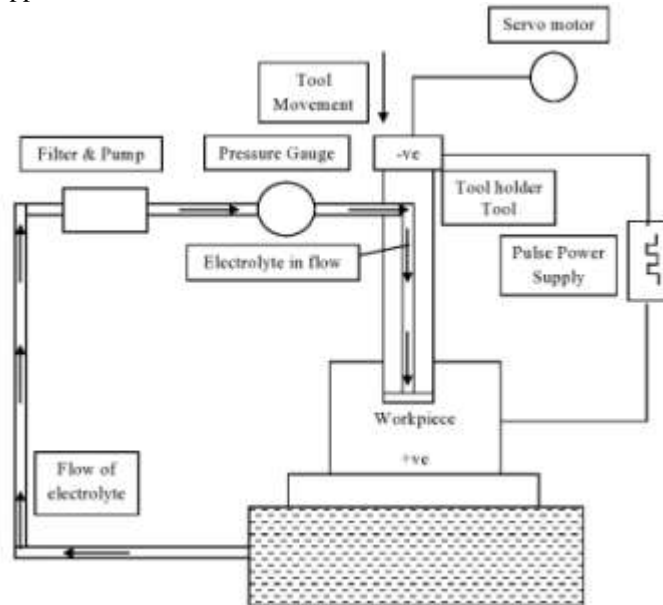


Fig. 1 Schematic diagram of various elements of ECM setup

Electrolyte

Electrolyte is a conducting fluid which plays a very vital role in electrochemical machining. An electrolyte in electrochemical machining completes electrical circuit allowing the passage of current (i.e. acts as a conductor), sustains the required electrochemical reactions and acts as a coolant and carries away the waste products. The selection of the electrolyte is based upon the work-piece material, the tool material and the application. Also, it must have a good chemical stability. Apart from these, it should be inexpensive, safe, and as non corrosive as possible.

Power Supply

Pulse DC power supply with low value of voltage and high value of current is used to minimize the loss of electricity. Current of the order of 50-40,000 A and voltage of order 4-30 V is generally applied to overcome the resistance at the gap.

MODELLING & SIMULATION

To machine the work piece into required shape, tool should be designed properly. The shape of the tool affects the critical parameters of machining and also affects the MRR.

Geometrical modelling: The modeling is done using PRO-E Design modeler. The model used for the simulation study under consideration in the present work is cylindrical shaped with a central through hole having a diameter of 2 mm and height 100 mm. The centre of the hole is fixed at (0, 0, 0) on XYZ coordinate. A cubical block having 100 mm length, 35 mm width and 5 mm height is used as work piece. Electrolyte used for this simulation is NaNO_3 solution. The electrolyte starts flowing with a constant diameter from the inlet of the tool. The complete physical model of work-piece-tool set up is as shown in figure 2.

Importing model to ANSYS: Model prepared in the ProE cannot be directly opened in the ANSYS. It has to be converted into a compatible format like IGES or STEP/STP for further processing. ProE model of the tool and work-piece assembly is firstly converted into STEP/STP format and then imported to ANSYS ICFD14.5.

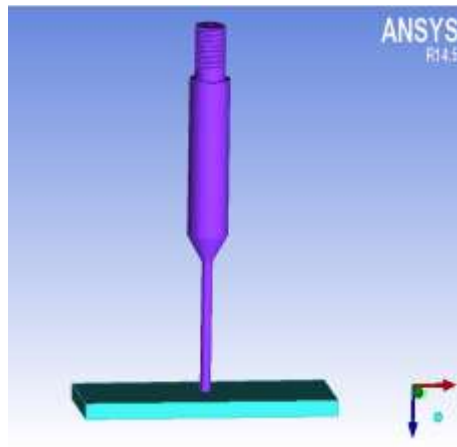


Fig.2: Physical model of work-piece-tool set up

Geometry checking: After importing the geometry to the ICFM CFD we repair the Geometry to check the errors like any incomplete surfaces, holes and gaps etc, by build diagnostic topology. These errors should be rectified as FLUENT does not tolerate such errors. After rectifying all the errors we can proceed further for part naming.

Part naming and material points: After importing the model from the Pro-E parts are assigned the name for identify. Material points are created to indicate the fluid volume or solid volume. Different names of the parts shown in the model tree. This fig 3 shows the different parts and their names.

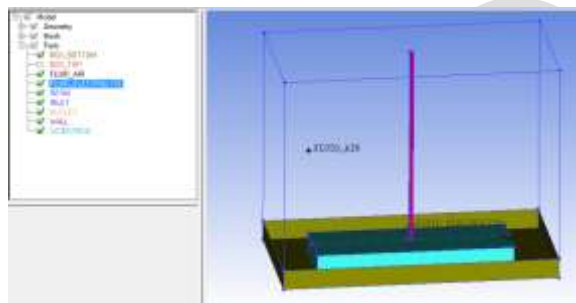


Fig.3: Model with part naming

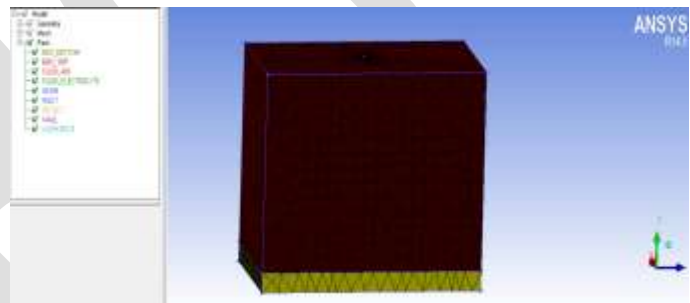


Fig.4: Meshed box model with part naming

Meshing: Meshing is used to discretizing a spatial domain in to simple geometric elements such as triangles (in 2D) or tetrahedral (in 3D) for getting the numerical solution. After importing the geometry and part naming we set the parameters for meshing. Firstly we have to decide which type of meshing we are going to do (a) Structured mesh, or (b) Unstructured mesh based on the application and complexity of the geometry. In the present work unstructured mesh is used as the model is not too complex and it also takes less time for calculation and analysis. The quality of mesh is a relevant factor in the case of appropriate geometry of the model and accuracy of the results. This can be expressed in terms of orthogonal quality. If the value of orthogonal quality is > 0 , mesh quality is good and better results are obtained while if it is < 0 , mesh gives bad results. Tetrahedron elements are used for meshing the geometry as they provides more automatic solutions with ability to add mesh controls to improve accuracy in critical regions [17]. We select the part mesh set up to set the proper mesh size for different parts of the model for capturing the proper physic and important features involved in that. The box structure outside the tool work piece setup is generated to capture the air volume which is present in atmosphere.

Next important step was to create prism elements over the wall surface as the flow pattern of the electrolyte is to be analysed so layer is created only over the electrolyte fluid volume.

After meshing we check the mesh for the different kind of errors which can create problems at the time of analysis in FLUENT. Errors which can create problem at the time of analysis are as follows [17]:

- (a) Duplicate elements
- (b) Uncovered faces
- (c) Missing internal faces
- (d) Volume orientation
- (e) Surface orientation
- (f) Hanging elements
- (g) Multiple edges
- (h) Triangle boxes
- (i) Single edges
- (j) Non-manifold vertices
- (k) Unconnected vertices.

Errors related to multiple edges and unconnected vertices are ignored as they do not create any problem while importing the model to FLUENT.

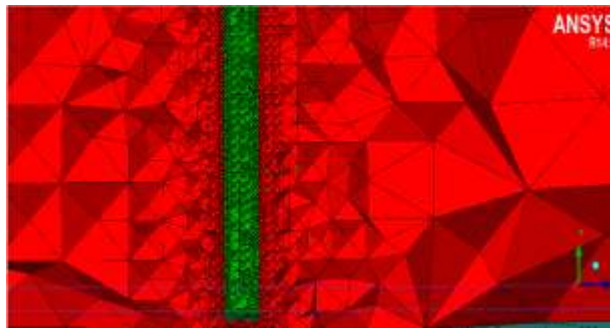


Fig.5: Volume mesh at cut plane

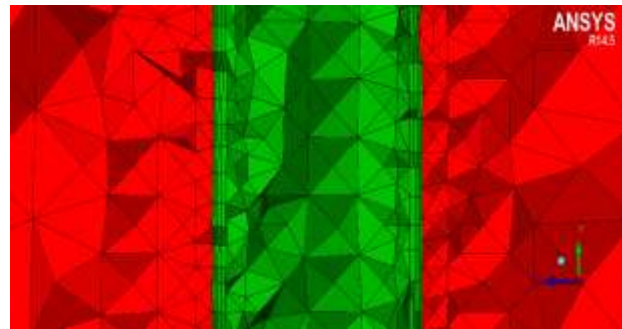


Fig.6: Prism layer at wall surface

Boundary conditions: Meshing done in ICEM is then imported in FLUENT in .msh file extension. Before setting the boundary conditions it is necessary to set proper dimensional units. So that proper results are achieved.

Model: In model setup we activate multiphase mode for volume of fluids, as we are considering two volumes: air and electrolyte. Energy equation is also activated as temperature profile is required in present work. As, we are working on 4000+ Reynolds number, So flow is turbulent. $k-\epsilon$ and $k-\Omega$ are two options available in turbulent flow model. $k-\epsilon$ model is selected for realizable wall function as it accurately predicts the spreading rate of both planar and round jets and also provides superior performance for flows involving rotation, boundary layers under strong adverse pressure gradients, separation, and recirculation.[17]

Material: In material setup we create material to be used as solid and fluid volumes as in our work copper and steel as solid material for tool and work-piece respectively and electrolyte and air as a fluid material are used. Air as a fluid volume is defined as it is present in the atmosphere and electrolyte as it circulates inside tool.

The input values for analysis are as:

For inlet zone we select type as pressure-inlet and box bottom as pressure-outlet.

In inlet conditions the pressure of 1.0, 1.2 and 1.4 kg/cm^2 accordingly are inserted. In specification method we give intensity as 5 and hydraulic diameter as 0.02m. For inlet thermal conditions temperature of air is taken as ambient temperature i.e. 300 k.

The outlet is set as a interior type, box-bottom set as pressure-outlet, the gauge pressure at the outlet surface will be "0". In specification method we give backflow intensity as 5 and backflow hydraulic diameter as 0.02 m.

RESULTS AND DISCUSSIONS

This deals with the analysis of the results of the three models generated in ANSYS Fluent as modelling. It shows the crucial parameters affecting overall machining process of ECM in terms of contours from which we can predict the variation of these parameters in the IEG and their effects.

It also describes the various experimental results we have obtained from the experiment performed.

Critical parameters analyzed in simulation:

Volume Fraction Profile

Figures 7, 8 and 9 show the volume fraction profiles, generated at different pressure. The inlet pressure for this simulation study was taken as 1.0 kg/cm^2 , 1.2 kg/cm^2 and 1.4 kg/cm^2 respectively. The volume fraction contours shown are the volume fraction of sodium nitrate electrolyte between IEG.

As in figure the volume fraction of the electrolyte is higher at the center of the hole and decrease at the outer side. The value of the volume fraction for model at different pressure will be different.

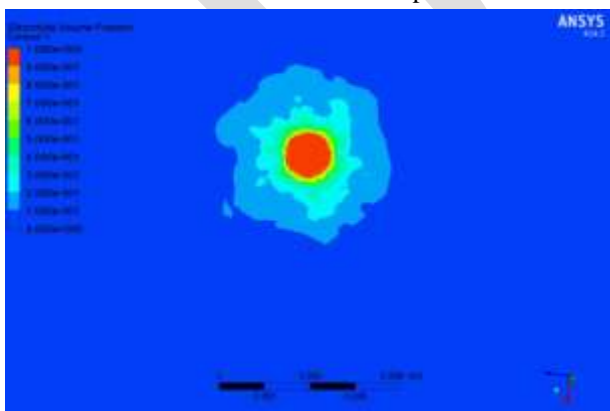


Fig.7: Volume fraction at pressure 1.0 kg/cm^2

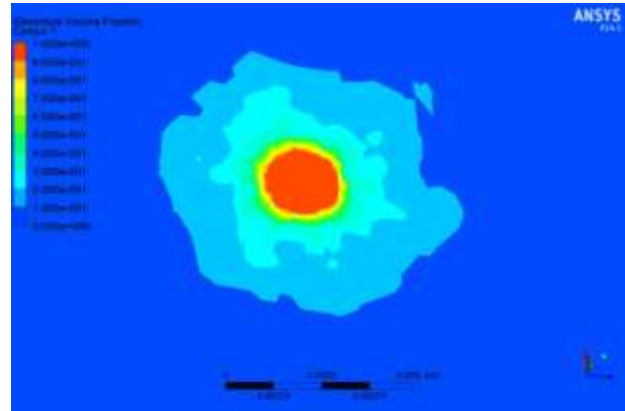


Fig.8: Volume fraction at pressure 1.2 kg/cm^2

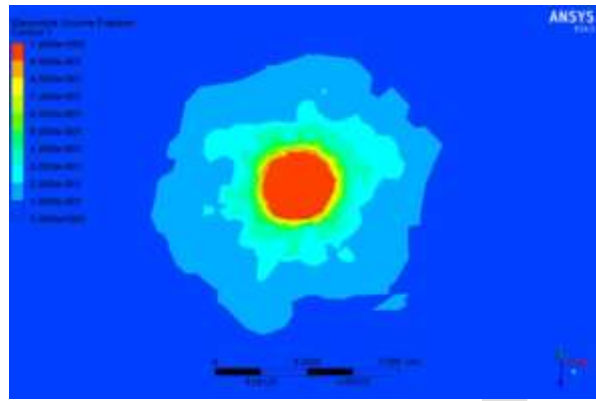


Fig.9: Volume fraction at pressure 1.4 kg/cm²

Velocity Profile

Figures 10, 11 and 12 show the velocity profile for model at inlet pressure 1.0 kg/cm², 1.2 kg/cm² and 1.4 kg/cm² respectively. The velocity profile at 1.0kg/cm² pressure is as shown in Fig. 10 which indicates that velocity of electrolyte increases from the hole to the boundary due to reduction in area of flow. The velocity of the electrolyte within the IEG is 10.03 m/s, which is less than the outlet velocity. So as the fluid flows towards the work-piece the velocity decreases. There is a slight change in velocity within IEG at different pressure.

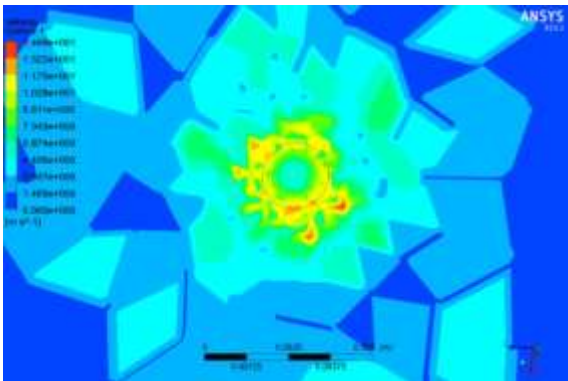


Fig.10: Velocity Profile at pressure 1.0 kg/cm²

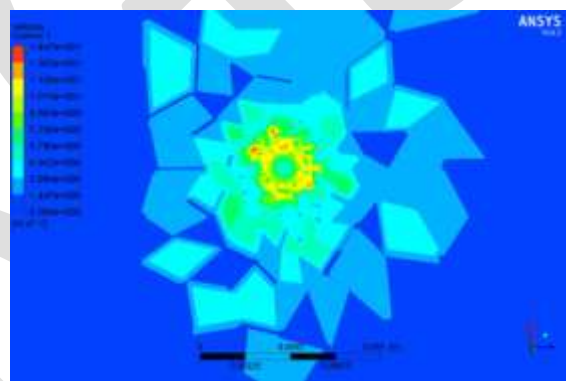


Fig.11: Velocity Profile at pressure 1.2 kg/cm²

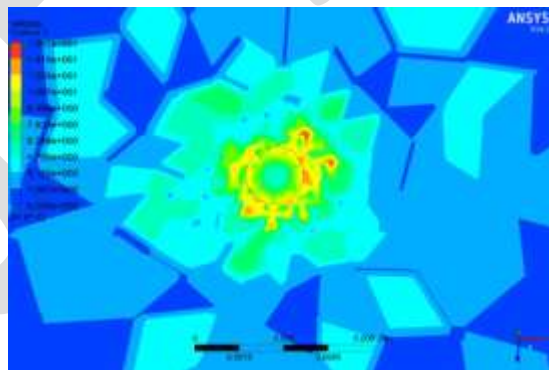


Fig.12: Velocity Profile at pressure 1.4 kg/cm²

Pressure Profile

Figures 13, 14 and 15 describes the pressure contours for model with different inlet pressure 1.0 kg/cm², 1.2 kg/cm² and 1.4 kg/cm² respectively in the inter electrode gap on the plane of work-piece.

The above pressure profiles describe the variation in pressure at the IEG on the plane of machining area. As all cases shows that pressure is higher at the center of the hole and decreases towards the boundary. The pressure increases from the inlet to outlet. The pressure within the IEG will be higher as compare to inlet pressure.

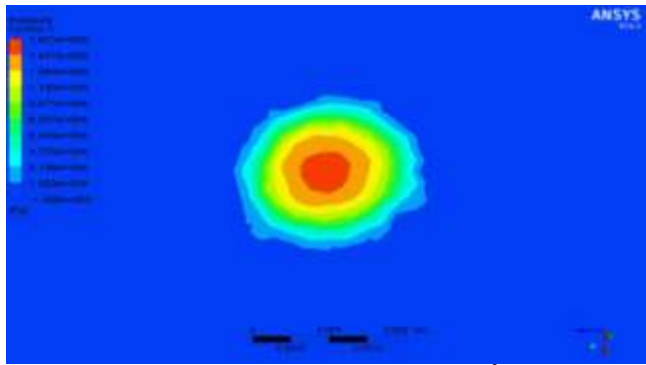


Fig.13: Pressure profile at inlet pressure 1.0 kg/cm²

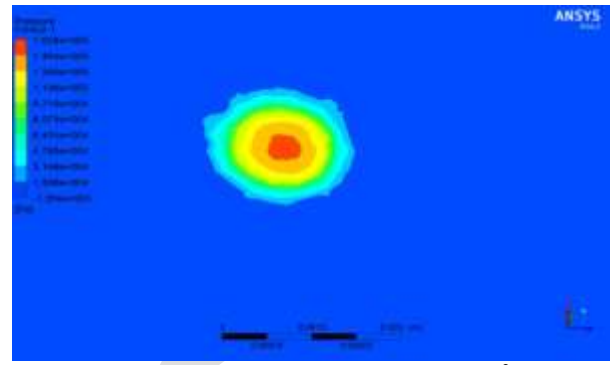


Fig.14: Pressure profile at inlet pressure 1.2 kg/cm²

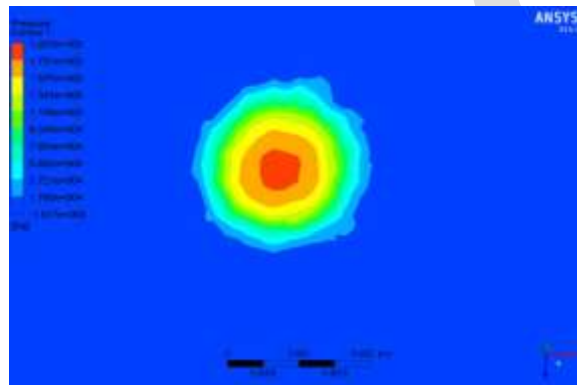


Fig.15: Pressure profile at inlet pressure 1.4 kg/cm²

Turbulent Kinetic Energy Profile

Figures 16, 17 and 18 show the turbulent kinetic energy contour within the IEG for model with different pressure.

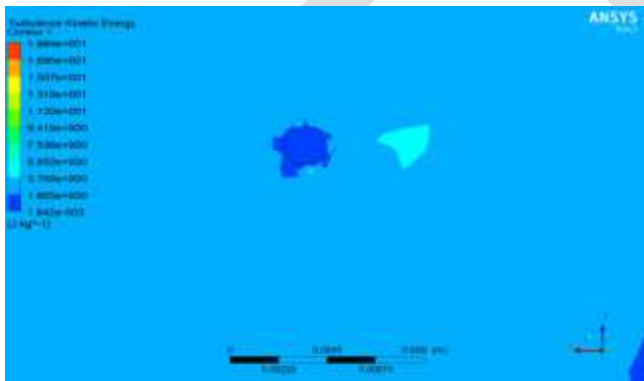


Fig.16: Turbulence kinetic energy profile at 1.0kg/cm²

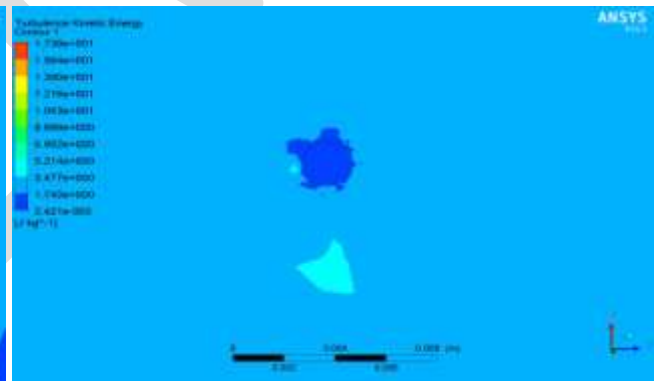


Fig.17: Turbulent kinetic energy profile at 1.2kg/cm²



Fig.18: Turbulence kinetic energy profile at pressure 1.4kg/cm²

Turbulence in the k-ε model depends on turbulent kinetic energy (k) and turbulent eddy dissipation (ε). Turbulence is directly related to the surface roughness. If the turbulence within the IEG is more, then the roughness of the machined surface will also be more. Turbulent kinetic energy determines the energy in the turbulence. Turbulent kinetic energy produced by fluid shear, friction or buoyancy or through external forcing at low frequency eddy scale. At 1.0kg/cm² pressure the kinetic energy values varies from 3.294×10⁻¹ m²/s² to 1.776×10 m²/s². In second case the variation of kinetic energy distribution is less than that of first case. The kinetic energy values varies from 3.264×10⁻¹ m²/s² to 1.75 m²/s². At 1.4kg/cm² pressure the kinetic energy values varies from 3.86×10⁻¹ m²/s² to 2.069 m²/s². This value is greater than that of case first and case second.

From the above discussion it can be observed that the value of kinetic energy within the IEG is very less at 1.2 kg/cm² pressure. So as shown in the figures 5.11 turbulent kinetic energy is less so there is less turbulence. And if the turbulence is low then we will get better machining surface.

Turbulent Eddy Dissipation Profile

Turbulent eddy dissipation gives the quantitative measurement of the turbulence. Figs. 19, 20 and 22 represent the profiles of turbulent eddy dissipation for model within the pressure range 1.0 -1.4 kg/cm².



Fig.19: Turbulent eddy dissipation at 1.0 kg/cm²



Fig.20: Turbulent eddy dissipation at 1.2 kg/cm²

At 1.0 kg/cm² pressure the value of eddy dissipation is varies from 2.22×10² m²/s³ to 1.0542×10⁴ m²/s³. In second case the variation of ‘ε’ distribution is less than that of case first. The ‘ε’ values are ranges from 2.19×10² m²/s³ to 1.0168×10⁴ m²/s³. At 1.4 kg/cm² pressure the value of eddy dissipation is varies from 2.81×10² m²/s³ to 1.3553 m²/s³ which is much greater than as compare to case first and second.

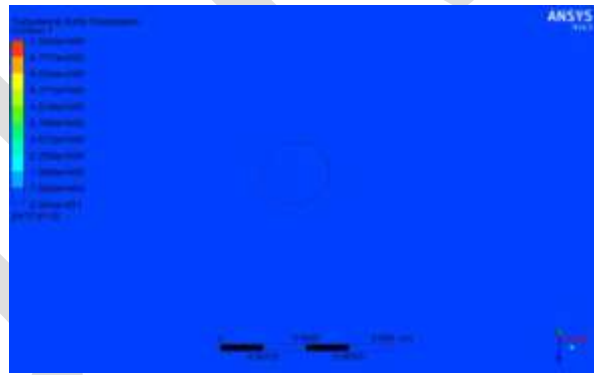


Fig.21: Turbulent eddy dissipation at 1.4 kg/cm²

It can be understood that at 1.2 kg/cm² pressure, the value of turbulent eddy dissipation is less within IEG.

Experimental results

After conducting the DOE as per Taguchi method using L9 orthogonal array for two repetitions following results/ responses are obtained for PECM.

Table 1: Result table

Test no	Response (repetition)		Test response total	Mean	S/N ratio
	1 st	2 nd			
E1	0.017	0.018	0.035	0.0175	-35.15
E2	0.046	0.052	0.098	0.049	-26.24
E3	0.023	0.018	0.041	0.0205	-33.95

E4	0.038	0.042	0.080	0.040	-31.95
E5	0.072	0.075	0.147	0.0735	-22.67
E6	0.033	0.039	0.072	0.036	-28.96
E7	0.037	0.032	0.069	0.0345	-29.31
E8	0.039	0.042	0.081	0.0405	-27.86
E9	0.063	0.058	0.121	0.0605	-24.38

Mean change in MRR

$$\Sigma A_1 = 0.035 + 0.098 + 0.041$$

$$\Sigma A_2 = 0.080 + 0.147 + 0.072$$

$$\Sigma A_3 = 0.069 + 0.081 + 0.121$$

Dividing ΣA_1 , ΣA_2 and ΣA_3 by 3×2 (i.e. three factor combinations and two repetitions), the mean change in MRR under the conditions A_1 , A_2 and A_3 was obtained. Thus;

$$A_1 = 0.174 / 6 = 0.029$$

$$A_2 = 0.298 / 6 = 0.0498$$

$$A_3 = 0.0270 / 6 = 0.045$$

Similarly calculating the mean change in MRR under the conditions $B_1, B_2, B_3, C_1, C_2, C_3$.

Signal to Noise Ratio

Taguchi method stresses the importance of studying the response variation using the signal -to- noise (S/N) ratio, resulting in minimization of quality characteristic variation due to uncontrollable parameter. The metal removal rate was considered as the quality characteristic with the concept of "the larger-the-better". The S/N Ratio for the larger-the-better is:

$$S/N = -10 \cdot \log(\text{mean square deviation})$$

$$S/N \text{ Ratio} = -10 \log_{10} \left[\frac{1}{n} \sum_{j=1}^n y_j^2 \right]$$

Larger is better (S/N) Ratio is used when there is no predetermined value for the target ($T = \infty$), and larger the value of the characteristics, the better the MRR. S/N Ratio and mean change under the condition A_1, A_2, \dots, C_2 and C_3 were calculated and presented in table 2.

Table 2: Mean change and S/N ratio for individual factors

Factor	Total result	Mean change	S/N Ratio
A1	0.174	0.029	-31.78
A2	0.298	0.0498	-27.86
A3	0.0270	0.045	-27.18
B1	0.1836	0.0306	-32.13
B2	0.3258	0.0543	-25.59
B3	0.234	0.039	-29.10
C1	0.1878	0.0313	-29.49
C2	0.298	0.0498	-27.52
C3	0.2568	0.0428	-28.64

Main effect plots

The main effect plots of MRR vs. Voltage, MRR vs. Feed rate and MRR vs. electrolyte pressure and S/N Ration vs. voltage, S/N Ratio vs. feed rate and S/N Ratio vs. electrolyte pressure for all the values obtained from MINITAB are as shown in the Figs. 22, 23, 24 and 25.

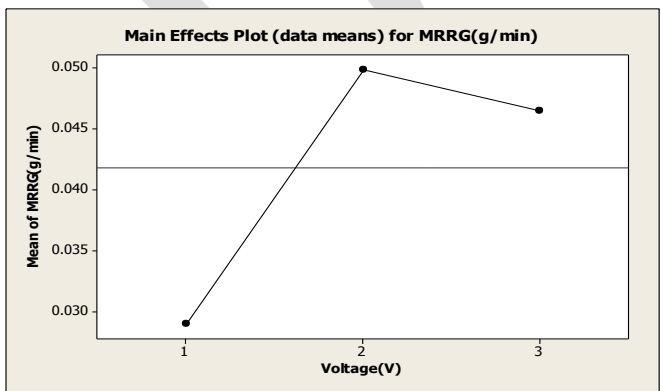


Fig.22: Effect of voltage on MRR

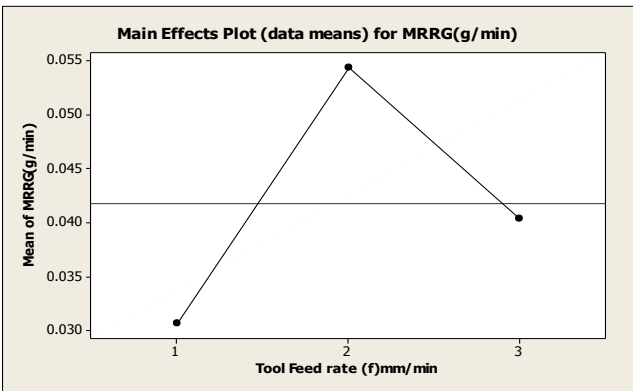


Fig.23: Effect of tool feed rate on MRR

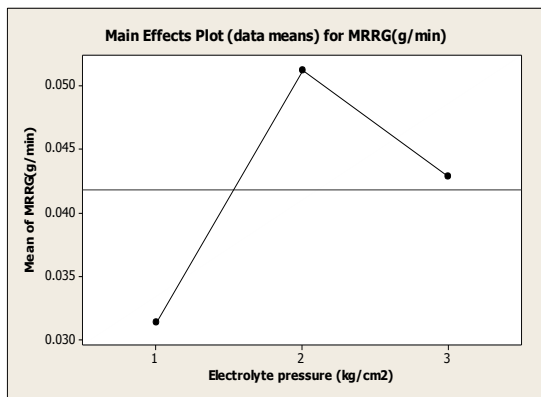


Fig.24: Effect of electrolyte pressure on MRR

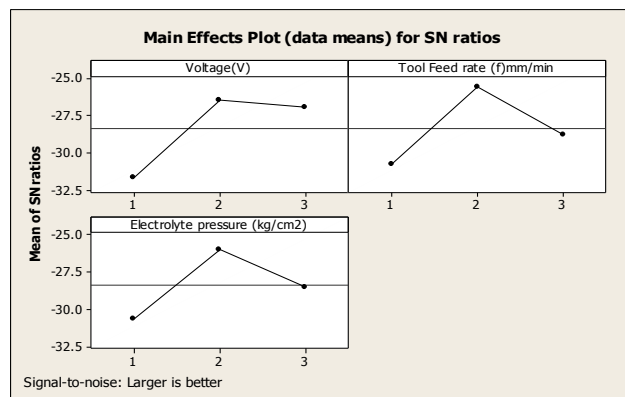


Fig.25: Effect of process parameters on S/N Ratio

Analysis Of Variance

The relative magnitude of the effect of different factors can be obtained by the decomposition of variance, called Analysis of Variance (ANOVA).

Overall Mean = 0.0413

Total Sum Of Square = SSTO = 0.005172,

Treatment Sum Of Square = SSTR_A = 0.001423,

SSTR_B = 0.001732,

SSTR_C = 0.001047,

Total Treatment Sum of Square = 0.004202

Error Sum Of Square = SSE = 0.00097

As we know that, SSTO = SSTR + SSE

SSTO = 0.004202 + 0.00097 = 0.005172 (verified)

Table.3: ANOVA Table

Parameter	DOF	SS	V	F	P (%)
A(Voltage)	2	0.001423	0.000711 5	7.12	27.51
B(Feed rate)	2	0.001732	0.000866	8.66	33.48
C (Pressure)	2	0.001047	0.000523 5	5.23 5	20.24
E (Error)	9	0.00097	0.0001	1	18.75
Total	15	0.005172			

In the ANOVA, the F-ratio is used to determine the significance of the factor. Percent (%) is defined as the significance rate of the process parameters on the metal removal rate. The percent number shows that the applied voltage, feed rate and electrolyte concentration have significant effect on the MRR. It can be observed from table that applied voltage (A), feed rate (B) and electrolyte pressure (C) affect the material removal rate by 27.51%, 33.48% and 20.24% in the pulse electrochemical machining of SS 3041 respectively.

CONCLUSIONS

Three dimensional two phase flow pattern analysis of electrochemical machining with circular (hollow) tool provides fundamental idea of velocity distribution, pressure pattern, turbulence etc. in the IEG. A cubical stainless steel work piece, circular copper tool and 15% sodium nitrate solution as electrolyte were considered in this analysis. Tool was modeled using Design Modeler of PRO-E and analyzed in ANSYS FLUENT 14.5. To get consistent and good results, model was meshed with Fine mesh resolution. Model is analyzed with inlet pressure of 1.0 kg/cm², 1.2 kg/cm² and 1.4 kg/cm² respectively.

Major conclusions:

- 1) The flow velocity decreases when electrolyte moves towards the work-piece and it increases at the outlet.
- 2) Turbulent kinetic energy and turbulent eddy dissipation rate profile exhibits higher value of turbulence at pressure 1.0 kg/cm² and 1.4 kg/cm² whereas at 1.2 kg/cm² pressure, turbulence is almost negligible.
- 3) The MRR is maximum affected by the tool feed rate followed voltage and least affected by the electrolyte pressure.
- 4) The optimized results A₂B₂C₂ gives the better material removal rate (MRR).

5) Hence, from the computational simulation and experimental results it was found that 1.2 kg/cm² is a optimum value for pressure .

REFERENCES:

- [1] Usharani Rath “Two phase flow analysis in electrochemical machining for l-shaped tool: A CFD APPROACH”. *M.tech project report (2013)*. National Institute of Technology, Rourkela, Odisha, India.
- [2] Baburaj, M. “CFD analysis of flow pattern in electrochemical machining for L-shaped tool”. *M.Tech project report (2012)*. National Institute of Technology, Rourkela, Odisha, India.
- [3] Benedict, Gary F. *Nontraditional Manufacturing Processes*, Marcel Dekker, Inc. 270 Madison Avenue, New York.
- [4] Ghosh, A. and Mallik, A.K., (2010). *Manufacturing Science Second Edition*, East- West Press Private Limited, New Delhi, India
- [5] Sekar T., Marappan R “Improving Material Removal Rate of Electrochemical Machining by Using Rotating Tool”
- [6] H. S. Beravala1, R. S. Barot, A. B. Pandey, G. D. Karhadkar (2011) “Development of Predictive Mathematical model of process parameters in ElectroChemical Machining Process”. *National conference on recent trends in engineering & technology*.
- [7] Rama Rao. S, Padmanabhan. G (2012) “Application of Taguchi methods and ANOVA in optimization of process parameters for metal removal rate in electrochemical machining of Al/5%SiC composites”. *International journal of engineering research and applications*, Vol. 2, pp. 192-197.
- [8] Suresh H. Surekar, Sudhir G. Bhatwadekar, Wasudev G. Kharche, Dayanand S. Bilgi (2012) “Determination Of Principle Component Affcting Material Removal Rate In Electrochemical Machining process”. *International journal of engineering science and technology*, Vol. 4, pp. 2402-2408.
- [9] J. Pattavanitch, S. Hinduja, J. Atkinson (2010) “Modelling of the electrochemical machining process by the boundary element method”. *CIRP Annals – Manufacturing technology*, Vol. 59, pp. 243-246.
- [10] M.H. Wanga, D. Zhub (2009) “Simulation of fabrication for gas turbine blade turbulated cooling hole in ECM based on FEM”. *Journal of material processing technology*, Vol. 209, pp. 1747-1751.
- [11] Mohan Sen, H.S. Shan (2005) “A review of electrochemical macro- to micro-hole drilling processes”. *International Journal of Machine Tools & Manufacture*, Vol. 45, pp. 137–152.
- [12] Evgueny I. Filatov (2001)“The numerical simulation of the unsteady ECM process”. *Journal of Materials Processing Technology*, Vol. 109 pp. 327-332.
- [13] Jerzy Kozak (2001)“Computer simulation system for electrochemical shaping”. *Journal of Materials Processing Technology*, Vol. 109, pp. 354-359.
- [14] Upendra Behera , P.J. Paul , S. Kasthuriengan , R. Karunanithi , S.N. Ram , K. Dinesh , S. Jacob () “CFD analysis and experimental investigations towards optimizing the parameters of Ranque–Hilsch vortex tube”.
- [15] Rui Wu, Danwen Zhang and Juan Sun (2011) “3-D Flow Field of Cathode Design for NC Precision Electrochemical Machining Integer Impeller Based on CFD”. *Research journal of applied sciences, engineering and technology*, Vol. 3, pp.1007-1013.
- [16] Krishna Mohan Singh1, R. N. Mall (2013) “Analysis Of Optimum Corner Radius Of Electrolyte Flow Path In ECM Using CFD”. *International journal of engineering research & technology*, Vol. 2, pp. 617-635.
- [17] Sian, S. “CFD analysis of flow pattern in electrochemical machining”. *B.Tech. Project Report (2011)*, National Institute of Technology Rourkela, Odisha, India.
- [18] Ansys Training Manual Inventory Number: 002600, 1st Edition ANSYS Release: 12.0, published date: 28April 2009.
- [19] Product Data Sheet, AK Steel , UNS S30400/UNS S30403